Article

Theoretical and Experimental Investigations on the Reactions of Positively Charged Phenyl Radicals with Aromatic Amino Acids

Yiqun Huang, and Hilkka Kenttmaa

J. Am. Chem. Soc., **2005**, 127 (21), 7952-7960• DOI: 10.1021/ja044314o • Publication Date (Web): 04 May 2005

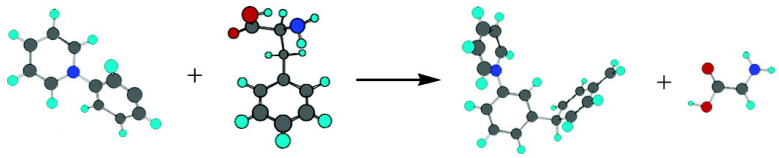

More About This Article

Additional resources and features associated with this article are available within the HTML version:

- Supporting Information
- Links to the 1 articles that cite this article, as of the time of this article download
- Access to high resolution figures
- Links to articles and content related to this article
- Copyright permission to reproduce figures and/or text from this article

View the Full Text HTML

J|A|C|S
ARTICLES
Published on Web 05/04/2005

Theoretical and Experimental Investigations on the Reactions of Positively Charged Phenyl Radicals with Aromatic Amino Acids

Yiqun Huang and Hilkka Kenttämaa*

Contribution from Brown Laboratories, Department of Chemistry, Purdue University, 425 Central Drive, West Lafayette, Indiana 47907-2018

Received September 17, 2004; E-mail: hilkka@purdue.edu

Abstract: The chemical behavior of positively charged phenyl radicals 3-dehydro-*N*-phenylpyridinium (**a**), *N*-(3-dehydro-5-chlorophenyl)pyridinium (**b**), and *N*-(3-dehydrophenyl)pyridinium (**c**) toward L-tyrosine, phenylalanine, and tryptophan was investigated in the gas phase both theoretically by performing molecular orbital calculations and experimentally by using FT/ICR mass spectrometry. All radicals react with phenylalanine and tryptophan nearly at the collision rate. The overall reactivity of the radicals toward tyrosine follows the order **a** > **b** > **c**, which is consistent with the electron affinity (EA) ordering of the radicals. The higher the electrophilicity (or EA) of the radical, the greater the reactivity. As expected, all radicals abstract a hydrogen atom from all of the amino acids. However, the most electrophilic radical **a** was also found to react with these amino acids via NH_2 abstraction. A new reaction observed between radicals **a**−**c** and aromatic amino acids is the addition of the radical to the aromatic ring of the amino acid followed by Cα−Cβ bond cleavage, which leads to side-chain abstraction by the radical.

Introduction

Radical attack on proteins is one of the main causes of oxidation damage of proteins.[1] Molecular level knowledge on these radical processes is limited because of the size and complexity of proteins. However, numerous investigations have been carried out on reactions of simple radicals (especially HO•) with free amino acids and small peptides.[2−7] These investigations provide useful insights into the possible mechanisms of the reactions of simple radicals with polypeptides and proteins. In aqueous solution, the HO• radical reacts with most amino acids and small peptides via hydrogen abstraction, and with aromatic amino acids via addition.[1]

Carbon-based radicals (especially phenyl radicals) released by some drugs and antitumor antibiotics, such as the enediynes, are known to attack nucleic acids. However, enediyne chromophores and their apoproteins also have been found to agglomerate proteins.[8a] Therefore, it is also of importance to explore the reactions of carbon-based radicals with amino acids. Contrary to the situation of the HO• radical, very little is known about these reactions. To our best knowledge, the only reaction reported for a phenyl radical and an amino acid is hydrogen abstraction from the α carbon of glycine by 4-dehydrobenzoate.[8b]

All of the studies mentioned above were carried out in solution. One of the advantages of liquid-phase studies is that many sophisticated analytical techniques can be utilized, such as EPR[3] and NMR.[6] However, the intrinsic chemical reactivity of radicals toward amino acids cannot be studied in solution due to the perturbation caused by solvent. Therefore, gas-phase reactions of the positively charged phenyl radicals (including radicals **a**−**c**; Figure 1) with six aliphatic amino acids (glycine, alanine, valine, proline, cysteine, and methionine) were recently investigated by using FT-ICR mass spectrometry.[9] Positively charged, chemically inert groups were affixed to these phenyl radicals (to form so-called distonic ions[10]) to allow mass spectrometric manipulation and detection of the phenyl radicals and their reaction products. Positively charged phenyl radicals have been demonstrated[11] earlier to undergo gas-phase reactions characteristic of those of neutral phenyl radicals in solution, such as hydrogen abstraction and addition. For instance, positively charged phenyl radicals were found to abstract hydrogen from thiophenol and benzeneselenol, and add to phenol, aniline, and toluene.[11b] Therefore, these radicals can be used to model the chemical behavior of neutral phenyl

(1) Hawkins, C. L.; Davies, M. J. *Biochim. Biophys. Acta* **2001**, *1504*, 196−219.
(2) Nagy, I. Z.; Floyd, R. A. *Biochim. Biophys. Acta* **1984**, *790*, 238−250.
(3) Hawkins, C. L.; Davies, M. J. *J. Chem. Soc., Perkin Trans. 2* **1998**, 2617−2622.
(4) Bonifačić, M.; Armstrong, D. A.; Carmichael, I.; Asmus, K.-D. *J. Phys. Chem. B* **2000**, *104*, 643−649.
(5) Štefanić, I.; Bonifačić, M.; Asmus, K.-D.; Armstrong, D. A. *J. Phys. Chem. A* 2**001**, *105*, 8681−8690.
(6) Nukuna, B. N.; Goshe, M. B.; Anderson, V. E. *J. Am. Chem. Soc.* **2001**, *123*, 1208−1214.
(7) Bonifačić, M.; Štefanić, I.; Hug, G. L.; Armstrong, D. A.; Asmus, K.-D. *J. Am. Chem. Soc.* **1998**, *120*, 9930−9940.
(8) (a) Zein, N.; Reiss, P.; Bernatowicz, M.; Bolgar, M. *Chem. Biol*. **1995**, *2*, 451−455. (b) Braslau, R.; Anderson, M. O. *Tetrahedron Lett.* **1998**, *39*, 4227−4230.
(9) (a) Guler, L. Ph.D. Thesis, Purdue University, 2002. (b) Huang, Y.; Guler, L.; Heidbrink, J.; Kenttämaa, H. I. *J. Am. Chem. Soc.* **2005**, *127*, 3973−3978.
(10) Yates, B. F.; Bouma, W. J.; Radom, L. *J. Am. Chem. Soc.* **1984**, *106*, 5805−5808.
(11) (a) Heidbrink, J. L.; Ramirez-Arizmendi, L. E.; Thoen, K. K.; Guler, L.; Kenttämaa, H. I. *J. Phys. Chem. A* **2001**, *105*, 7875−7884. (b) Ramirez-Arizmendi, L. E.; Guler, L.; Ferra, J. J., Jr.; Thoen, K. K.; Kenttämaa, H. I. *Int. J. Mass Spectrom.* **2001**, *210/211*, 511−520.

10.1021/ja044314o CCC: $30.25

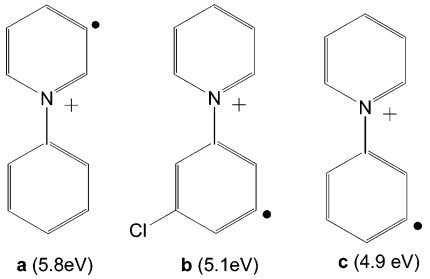

Figure 1. The structures of radicals **a**−**c** and their vertical electron affinities.[9]

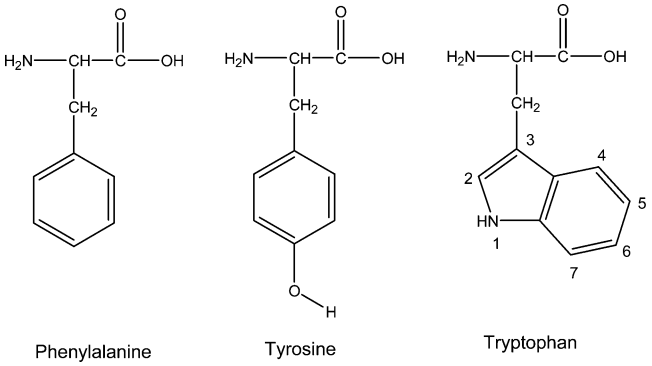

Figure 2. The structures of phenylalanine, tyrosine, and tryptophan.

radicals toward amino acids. The amino acids (with the exception of methionine) react with radicals **b** and **c** via exclusive hydrogen transfer, which was found to occur from the α carbon, the NH_2 group, and likely also from the side chain.[9] Radical **a**, however, also undergoes NH_2 abstraction. This novel reaction was assumed to occur via an addition−elimination mechanism and was attributed to the great electrophilicity of radical **a**.[9] Other novel reactions observed include SH abstraction from cysteine and SCH_3 abstraction from methionine. These findings inspired the present study. We report here on the unprecedented chemical behavior of radicals **a**−**c** toward the aromatic amino acids phenylalanine, tryptophan, and tyrosine (Figure 2).

Experimental Section

The experiments were carried out by using a Finnigan FTMS 2001 Fourier transform ion cyclotron resonance mass spectrometer (FT/ICR). The instrument contains a differentially pumped dual cell in a magnetic field produced by a 3.0 T superconducting magnet. The nominal base pressure was $<10^{-9}$ Torr, as maintained by two Edwards diffusion pumps (800 L/s), each backed with an Alcatel 2012 mechanical pump. The two cells of the instrument are separated by a metal wall called the conductance limit with a 2 mm hole in the center. All trapping plates were maintained at +2 V unless otherwise specified.

Samples were introduced into the instrument by using Varian leak valves, heated solids probes, pulsed valves, or batch inlet systems equipped with a variable leak valve. The nominal reagent pressures were measured with two ionization gauges, one located on each side of the dual cell.

The amino acids used in this study are L-phenylalanine, L-tyrosine, and L-tryptophan. All amino acids were obtained from Fluka Biochemika. The positively charged phenyl radicals used in the present work are 3-dehydro-*N*-phenylpyridinium (**a**), *N*-(3-dehydro-5-chlorophenyl)pyridinium (**b**), and *N*-(3-dehydrophenyl)pyridinium (**c**). The reagents used for the generation of these phenyl radicals are chlorobenzene, bromobenzene, iodobenzene, 1,3-diiodobenzene, and 1,3-dichloro-5-iodobenzene (all from Sigma-Aldrich), as well as 3-iodopyridine (KARL industries Inc.) and pyridine (Mallinckrodt Specialty Chemicals). All of these chemicals were used without further purification.

Charged phenyl radicals were generated using a procedure reported earlier.[12] For the preparation of radical **a**, chlorobenzene (or bromobenzene or iodobenzene) was introduced at a nominal pressure of 6.0×10^{-8} to 1.1×10^{-7} Torr into one side of the dual cell by using a batch inlet system. 3-Iodopyridine was introduced at the same nominal pressure into the same cell through a Varian leak valve. For the generation of radicals **b** and **c**, the halobenzene precursors (1,3-dichloro-5-iodobenzene for radical **b**, and 1,3-diiodobenzene for radical **c**) were introduced through a Varian leak valve, while pyridine was introduced through a batch inlet into the same cell at the same nominal pressure. The mixture was subjected to electron ionization that resulted in the formation of halobenzene radical cations. Typical electron ionization conditions were 20 eV electron energy, 5 μA emission current, and 50 ms ionization time. The halobenzene radical cations were allowed to react with pyridine (for radicals **b** and **c**) or 3-iodopyridine (for radical **a**) for 4−5 s. The *ipso*-substitution of a halogen atom yielded abundant substituted halobenzene ions.

The substituted halobenzene ions, generated in one side of the dual cell, were transferred into the other side by grounding the conductance limit plate for about 175−180 μs, which allowed the ions to pass through the 2 mm hole in the center of the plate. The transferred ions were allowed to cool for about 1 s via IR emission and by collisions with the neutral molecules present in this cell (the reagent to be used in the final stage of the experiment). The substituted halobenzene ions were isolated by ejecting all unwanted ions via the application of a stored-waveform inverse Fourier transform[13] (SWIFT) excitation pulse to the cell. The ions were subjected to homolytic carbon−halogen bond cleavage to form a radical site by using sustained off-resonance irradiated collision-activated dissociation (SORI-CAD).[14] SORI-CAD was implemented by introducing argon into the cell via a pulsed valve assembly (the nominal peak pressure in the cell was about 1×10^{-5} Torr) and collisionally activating the ions with argon for 0.5−1 s at a frequency 1 kHz higher than the cyclotron frequency of the ions. The charged phenyl radicals were cooled by providing about 400 ms time delay for IR emission, and for collisions with the neutral molecules present in the cell. Charged phenyl radicals were isolated by applying a SWIFT excitation pulse to the cell. The isolated charged phenyl radicals were allowed to react with an amino acid for a variable period of time (typically 10−160 s). The amino acids were introduced via a heated solids probe at about 10^{-8} Torr. Detection was performed by using "chirp" excitation of 124 V_{p-p} amplitude, 2.7 MHz bandwidth, and 3.2 kHz/ms sweep rate. All of the spectra are the average of 15 transients, which were recorded as 64k data points and subjected to one zero fill prior to Fourier transformation. Each reaction spectrum was background corrected by using a procedure described previously.[15]

Primary product ions were identified on the basis of their fixed relative abundances (branching ratios) at short reaction times. By assuming pseudo-first-order kinetics, the second-order rate constant of reactions (k_{exp}) was obtained from a semilogarithmic plot of the relative abundance of the reactant ion versus time. A parametrized trajectory theory[16] was employed to calculate the collision rate constants (k_{coll}). The reaction efficiencies are given as k_{exp}/k_{coll}. The accuracy of the rate constant measurements is estimated to be 50%, while the precision is better than 10%. The greatest uncertainty arises from the pressure measurement in the cell. The pressure readings of the ion gauges

(12) Heidbrink, J. L.; Thoen, K. K.; Kenttämaa, H. I. *J. Org. Chem.* **2000**, *65*, 645−651.
(13) Chen, L.; Wang, T.-C. L.; Ricca, T. L.; Marshall, A. G. *Anal. Chem.* **1987**, *59*, 449−454.
(14) Gauthier, J. W.; Trautman, T. R.; Jacobson, D. B. *Anal. Chim. Acta* **1991**, *246*, 211−225.
(15) Leeck, D. T.; Stirk, K. M.; Zeller, L. C.; Kiminkinen, L. K. M.; Castro, L. M.; Vainiotalo, P.; Kenttämaa, H. I. *J. Am. Chem. Soc.* **1994**, *116*, 3028−3038.
(16) Su, T.; Chesnavich, W. J. *J. Chem. Phys.* **1982**, *76*, 5183−5185.

(located remote from the cell) were corrected for their sensitivity toward each neutral reagent[17,18] and for the pressure gradient between the cell and the ion gauge. The latter correction factor was obtained for each neutral reagent by measuring rates of exothermic proton-transfer reactions (with protonated acetone) assumed to occur at the collision rate.

The potential energy surfaces for the addition−elimination reaction pathways of radical **c** with phenylalanine and tyrosine were explored by performing density functional theory-based molecular orbital calculations by using the Gaussian 98 revision A.11 suite of programs.[19] The enthalpy changes (exothermicities) for the addition−elimination reactions were determined directly at absolute zero kelvin by optimizing the geometries of the reactants and products and calculating their corresponding electronic energies at the B3LYP/6-31G(d) level of theory. All optimized geometries were verified to be real local minima by performing frequency analysis (no imaginary frequencies). The corresponding zero-point vibrational energies (ZPVE) were calculated at the same level of theory and used to correct the electronic energies. The zero-point energies were scaled by multiplying by a scaling factor of 0.9804.[20] The geometries and energies of transition states along the addition−elimination pathways were determined by performing transition state calculations at the B3LYP/6-31G(d) +ZPVE level of theory. The transition states were verified as true first-order saddle points along the correct reaction coordinate by frequency analysis (one imaginary frequency corresponding to the vibration along the reaction coordinate that leads to the decomposition of transition state into products).

Results and Discussion

In this work, the chemical behavior of radicals **a**−**c** toward the three amino acids shown in Figure 2 was examined in the gas phase in a Fourier transform ion cyclotron resonance mass spectrometer. The radicals' reactivity is characterized by a measured reaction efficiency that is defined as the ratio of the second-order reaction rate constant to a calculated collision rate constant (see Experimental Section). Previous studies carried out in our laboratories have shown that a positively charged phenyl radical with a high vertical electron affinity usually displays high radical reactivity[11] ("vertical electron affinity" of a radical is defined here as the energy released when an extra electron is added to the radical site at a frozen radical geometry). In this study, radical **a** was found to be the most reactive (has greatest reaction efficiency) toward tyrosine, followed by radicals **b** and **c**. This reactivity ordering is consistent with the vertical electron affinity ordering of these radicals (EA = 5.8, 5.1, and 4.9 eV for radicals **a**, **b**, and **c**, respectively[9]). These EA values are high but not high enough to ionize the amino acids (the ionization energies of phenylalanine and tyrosine are 8.4 and 8.0 eV, respectively;[21] the ionization energy of tryptophan is unknown). Therefore, there is no electron transfer from the amino acids to the radicals. All radicals react very rapidly with all three amino acids. The radicals abstract hydrogen from all of the amino acids studied. A few other product ions are also formed, mainly via reactions with the aromatic ring of the amino acids. Only the fastest reactions are discussed below.

Table 1. Product Branching Ratios[a] Measured for the Reactions of L-Phenylalanine (MW = 165) with Radicals **a**−**c**

	product branching ratios (%)					
radical	hydrogen abstraction	adduct-X[b]	adduct-17	adduct	NH_2 abstraction	other ions
a	12	60	11	0	6	(*m*/*z* 181) 11
b	4	88	0	8	0	0
c	4	85	0	10	0	0

[a] Product branching ratios are the average values of several experiments. [b] X = $NH_2CH{\cdot}COOH$.

Reactions of Radicals a−c with Phenylalanine. Radicals **a**−**c** react with phenylalanine nearly at the collision rate (due to an unstable pressure of phenylalanine inside the FT-ICR cell, accurate reaction efficiencies could not be obtained). The product branching ratios for the reactions of radicals **a**−**c** with phenylalanine are given in Table 1. A mass spectrum measured after reaction of phenylalanine with radical **b** is shown in Figure 3. All radicals (**a**−**c**) abstract hydrogen from phenylalanine. However, the branching ratio of the hydrogen abstraction product is only about 10% or less. Radical **a** was found to abstract the NH_2 group of phenylalanine, because of its high electrophilicity (EA = 5.8 eV).[9] The predominant products of reactions of radicals **a**−**c** with phenylalanine are ions with a *m*/*z* value that is 74 units lower than that of the corresponding adduct. These ions can be formed via the addition of a radical to either the *ortho*- or the *para*-position of the phenyl ring, followed by Cα−Cβ bond cleavage to form a side-chain abstraction product. Feasible formation mechanisms for these side-chain abstraction products are illustrated in Figure 4. The *meta*- and *ipso*-addition likely yield the observed adducts because these adducts cannot dissociate via Cα−Cβ bond cleavage. The potential energy surfaces for the reactions of radical **c** and phenylalanine along the pathways of phenyl ring addition followed by Cα−Cβ bond cleavage were explored in this study at the B3LYP/6-31G(d) level of theory. The results are shown in Figures 5 and 6.

Similar to simple amino acids,[22−28] phenylalanine molecules can exist in numerous conformations. However, only one systematic gas-phase conformational study appears to have been published for phenylalanine.[29] The most stable conformation of phenylalanine reported in that study[29] was chosen as the initial amino acid backbone geometry for the preliminary conformational search of the addition intermediates in the present work. The addition intermediates were then subjected to full optimiza-

(17) Miller, K. J.; Savchik, J. A. *J. Am. Chem. Soc.* **1979**, *101*, 7206−7213.
(18) Bartmess, J. E.; Georgiadis, R. M. *Vacuum* **1983**, *33*, 149−153.
(19) Frisch, M. J.; Trucks, G. W.; Schlegel, H. B.; Scuseria, G. E.; Robb, M. A.; Cheeseman, J. R.; Zakrzewski, V. G.; Montgomery, J. A., Jr.; Stratmann, R. E.; Burant, J. C.; Dapprich, S.; Millam, J. M.; Daniels, A. D.; Kudin, K. N.; Strain, M. C.; Farkas, O.; Tomasi, J.; Barone, V.; Cossi, M.; Cammi, R.; Mennucci, B.; Pomelli, C.; Adamo, C.; Clifford, S.; Ochterski, J.; Petersson, G. A.; Ayala, P. Y.; Cui, Q.; Morokuma, K.; Malick, D. K.; Rabuck, A. D.; Raghavachari, K.; Foresman, J. B.; Cioslowski, J.; Ortiz, J. V.; Baboul, A. G.; Stefanov, B. B.; Liu, G.; Liashenko, A.; Piskorz, P.; Komaromi, I.; Gomperts, R.; Martin, R. L.; Fox, D. J.; Keith, T.; Al-Laham, M. A.; Peng, C. Y.; Nanayakkara, A.; Gonzalez, C.; Challacombe, M.; Gill, P. M. W.; Johnson, B.; Chen, W.; Wong, M. W.; Andres, J. L.; Gonzalez, C.; Head-Gordon, M.; Replogle, E. S.; Pople, J. A. *Gaussian 98*, revision A.11; Gaussian, Inc.: Pittsburgh, PA, 1998.
(20) Foresman, J. B.; Frisch, Æ. *Exploring Chemistry with Electronic Structure Methods*, 2nd ed.; Gaussian, Inc.: Pittsburgh, PA, 1996.
(21) Linstrom, P. J., Mallard, W. G., Eds. NIST Chemistry WebBook, NIST Standard Reference Database Number 69, March 2003, National Institute of Standards and Technology, Gaithersburg MD, 20899 (http://webbook.nist.gov).
(22) Jensen, J. H.; Gordon, M. S. *J. Am. Chem. Soc.* **1991**, *113*, 7917−7924.
(23) Stepanian, S. G.; Reva, I. D.; Radchenko, E. D.; Adamowicz, L. *J. Phys. Chem. A* **1999**, *103*, 4404−4412.
(24) Yu, D.; Rauk, A.; Armstrong, D. A. *J. Am. Chem. Soc.* **1995**, *117*, 1789−1796.
(25) O'Hair, R. A. J.; Bowie, J. H.; Gronert, S. *Int. J. Mass Spectrom. Ion* **1992**, *117*, 23−26.
(26) Shirazian, S.; Gronert, S. *THEOCHEM* **1997**, *397*, 107−112.
(27) Fernández-Ramos, A.; Cabaleiro-Lago, E.; Hermida-Ramón, J. M.; Martínez-Núñez, E.; Peña-Gallego, A. *THEOCHEM* **2000**, *498*, 191−200.
(28) Gronert, S.; O'Hair, R. A. J. *J. Am. Chem. Soc.* **1995**, *117*, 2071−2081.
(29) Snoek, L. C.; Robertson, E. G.; Kroemer, R. T.; Simons, J. P. *Chem. Phys. Lett.* **2000**, *321*, 49−56.

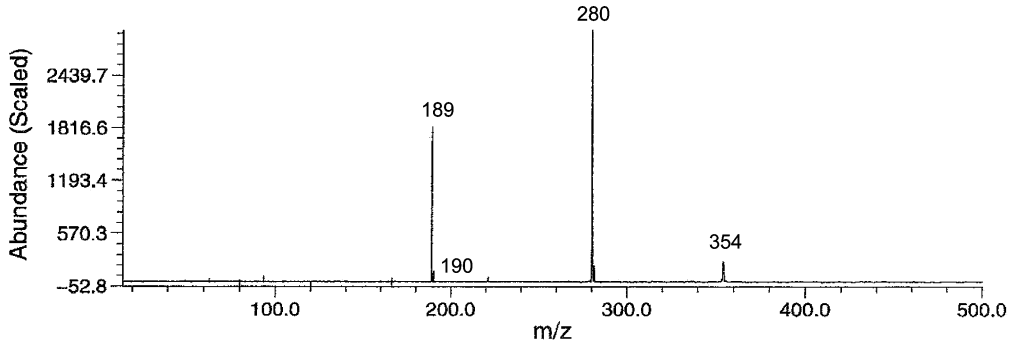

Figure 3. A mass spectrum obtained after 4 s reaction of phenylalanine with radical **b**. The *m*/*z* values for radical **b**, and the hydrogen abstraction, side-chain abstraction, and addition products are 189, 190, 280, and 354, respectively.

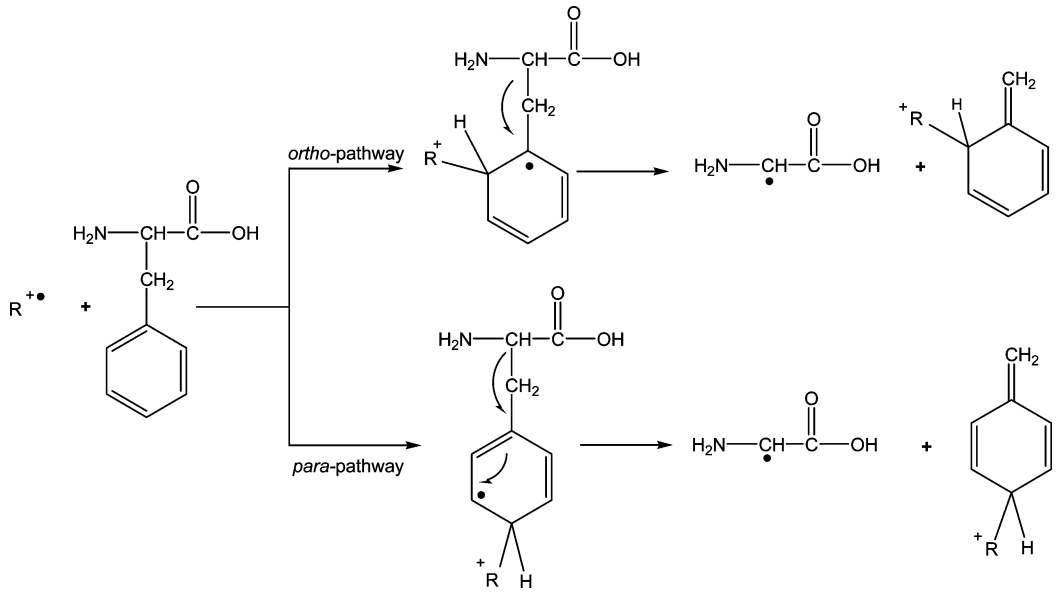

Figure 4. Possible mechanisms for the addition of radicals **a**−**c** (represented by $R^{+\bullet}$) to phenylalanine followed by side-chain abstraction.

tion at the B3LYP/6-31G(d) + ZPVE level. The transition states for the addition and dissociation steps were calculated at the B3LYP/6-31G(d) + ZPVE level of theory based on the knowledge of the fully optimized adduct geometries.

When radical **c** approaches phenylalanine along the *ortho*-addition pathway (Figure 5), the carbonyl oxygen of phenylalanine can approach the C−H bond of the pyridine ring adjacent to the nitrogen to form a weak C−H---O hydrogen bond. The hydrogen bonding helps to stabilize the transition state of the addition step. Consequently, the addition transition state is about 9.6 kcal/mol lower in energy than the separated reactants. Similar interactions stabilize the adduct and the dissociation transition state. The formation of the adduct is exothermic by 34.0 kcal/mol with respect to the separated reactants. The transition state for the dissociation of the adduct via Cα−Cβ cleavage is 4.4 kcal/mol lower in energy than the separated reactants, which leads to a 29.6 kcal/mol energy barrier. Under ICR conditions, the total energy and angular momentum of the system are conserved.[30−32] Therefore, this energy barrier can be overcome, and a product-like ion−molecule complex is formed that finally decomposes into the two products. The overall enthalpy change for the reaction is about −4.1 kcal/mol.

The potential energy surface calculated for the *para*-addition is very similar to that for the *ortho*-pathway. Radical **c** can approach phenylalanine in such a manner that hydrogen bonding stabilizes the transition state for addition, the adduct, and the transition state for dissociation. The addition transition state is about 9.1 kcal/mol lower in energy than the separated reactants. The formation of the adduct is about 31.1 kcal/mol exothermic. A 26.2 kcal/mol energy barrier needs to be overcome for the adduct to dissociate. This can be achieved because of the conservation of the total energy of the system. The total enthalpy change of the addition−dissociation process is about −8.2 kcal/mol.

Reactions of Radicals a−c with Tyrosine. The overall reaction efficiencies and the product branching ratios for the reactions of radicals **a**−**c** with tyrosine are shown in Table 2. Radical **a** is more reactive than radicals **b** and **c**, presumably because of its larger electrophilicity, which is reflected in its electron affinity.[9] Hydrogen abstraction was observed for all radicals. Stable addition products are more abundant for tyrosine than for phenylalanine. A possible reason for the unexpected stability of the adduct is that tyrosine should be a better IR emitter than phenylalanine because of the presence of the hydroxyl functionality. Therefore, the adducts of tyrosine may get faster stabilized by releasing excess internal energy via IR emission. The reactions of radicals **a**−**c** with tyrosine are not

(30) Olmstead, W. N.; Brauman, J. I. *J. Am. Chem. Soc.* **1977**, *99*, 4219−4228.
(31) Asubiojo, O. I.; Brauman, J. I. *J. Am. Chem. Soc.* **1979**, *101*, 3715−3724.
(32) Dodd, J. A.; Brauman, J. I. *J. Phys. Chem.* **1986**, *90*, 3559−3562.

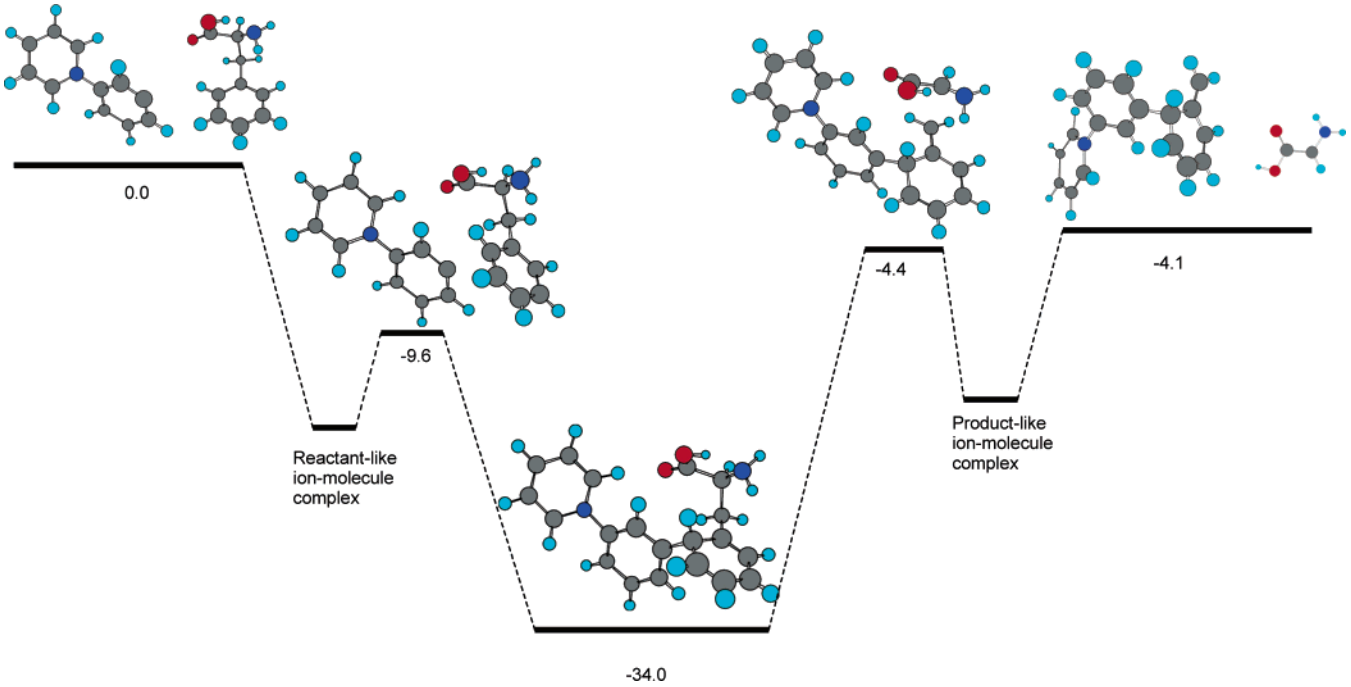

Figure 5. The potential energy surface (not scaled) for the addition of radical **c** to the *ortho*-position of phenylalanine, followed by side-chain abstraction, as calculated at the B3LYP/6-31G (d)+ZPVE level of theory. All numbers are in kcal/mol.

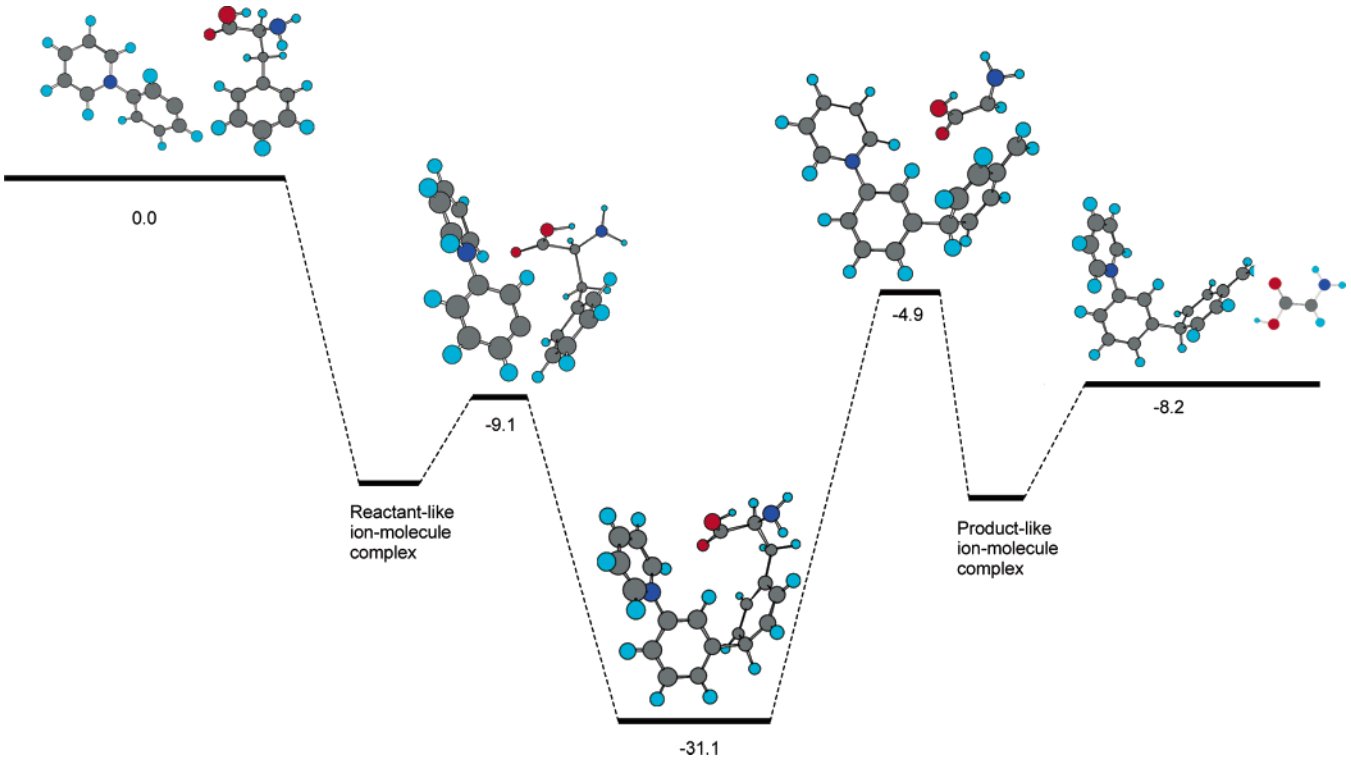

Figure 6. The potential energy surface (not scaled) for the addition of radical **c** to the *para*-position of phenylalanine, followed by side-chain abstraction, as calculated at the B3LYP/6-31G (d)+ZPVE level of theory. All numbers are in kcal/mol.

dominated by addition followed by side-chain abstraction as they are for phenylalanine (this reaction only accounts for less than 10% of the total products in the case of tyrosine). Instead, adduct-OH is the major product for radical **a**. An equal preference to form a stable adduct, adduct-OH, and hydrogen abstraction products was observed for radicals **b** and **c**. Just as for phenylalanine, both *ortho*- and *para*-positions in tyrosine can be subject to addition and subsequent side-chain abstraction. The adduct-OH ion, on the other hand, can only be formed upon *para*-addition. Possible mechanisms for addition and subsequent side-chain elimination or OH loss are shown in Figure 7.

To explain the discrepancy between the product branching ratios of tyrosine and phenylalanine, the potential energy surfaces for three reaction pathways (*ortho*-addition followed by side-chain abstraction, and *para*-addition followed by either side-chain abstraction or OH loss) were calculated for radical **c**

Table 2. Overall Reaction Efficiencies and Product Branching Ratios[a] Measured for the Reactions of L-Tyrosine (MW = 181) with Radicals **a**−**c**

		product branching ratios (%)						
radical	overall efficiency (%)	hydrogen abstraction	adduct-X[b]	adduct-OH	adduct-H	adduct	NH_2 abstraction	other ions
a	62	16	6.5	40	11	4	8	(*m*/*z* 197, 248) 15
b	40	28	10	36	0	26	0	0
c	26	31	7	26	0	36	0	0

[a] Reaction efficiencies and product branching ratios are the average values of several experiments. [b] X = $NH_2CH{\cdot}COOH$.

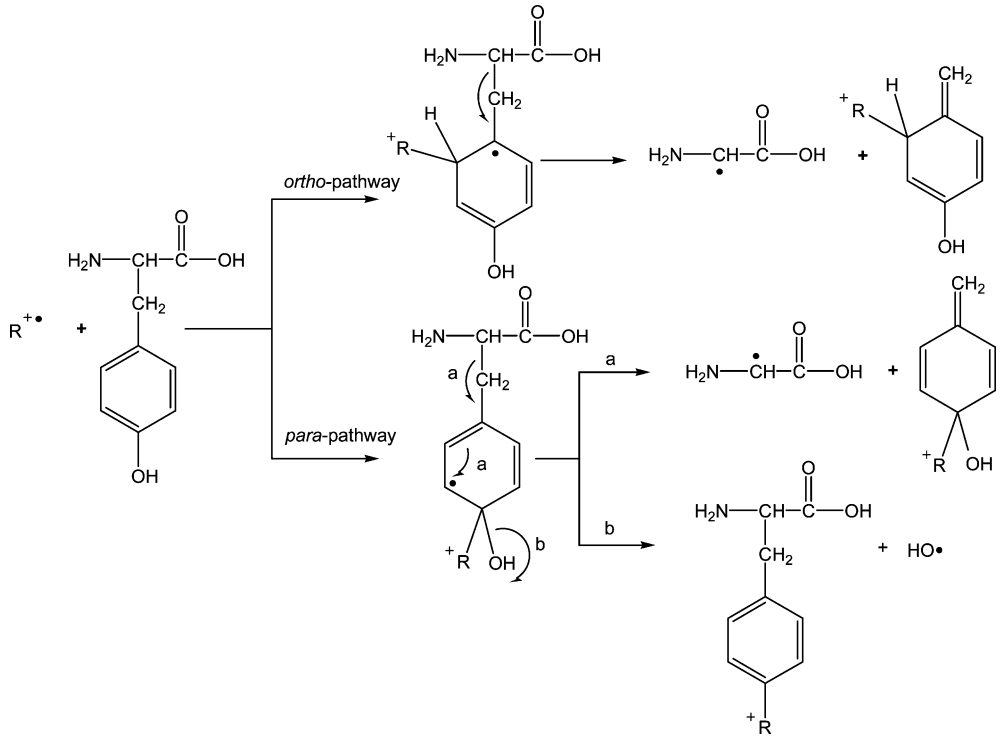

Figure 7. Possible mechanisms for the addition of radicals **a**−**c** (represented by $R^{+\bullet}$) to tyrosine followed by side-chain abstraction or OH loss.

at the B3LYP/6-31G(d) + ZPVE level of theory. To the best of our knowledge, no systematic conformational studies have been reported for tyrosine in the gas phase. However, it has been pointed out that the most stable conformers of all aromatic amino acids are similar, and they enjoy a stabilizing interaction between the amino group and the π system of the aromatic ring.[29] Therefore, a three-dimensional structure similar to the most stable conformer of phenylalanine was chosen as the starting structure of tyrosine in this study. The full optimization of this structure showed that in the most stable conformation of tyrosine, the hydroxyl group lies almost on the plane of the phenyl ring, and the hydroxyl hydrogen points into the same direction as the carboxylic group (see Figure 2). A preliminary conformational search similar to that carried out for phenylalanine was performed for tyrosine to get preliminary information on the most favored structures of the addition intermediates. Based on the information obtained, full optimization of the adducts and transition states was performed. The potential energy surfaces calculated for the three reaction pathways mentioned above are shown in Figures 8−10. When radical **c** approaches tyrosine along the *ortho*-addition pathway (Figure 8), an ion−dipole interaction and a weak hydrogen bond stabilize the addition transition state that lies about 9.3 kcal/mol lower in energy than the separated reactants. These intramolecular interactions are also present in the adduct and the dissociation transition state. The adduct formation is highly exothermic. The adduct lies 33.7 kcal/mol lower in energy than the separated reactants. The transition state for the dissociation of the adduct via Cα−Cβ cleavage is about 4.4 kcal/mol lower in energy than the reactants, resulting in a 29.3 kcal/mol energy barrier. The overall enthalpy change for the entire reaction is about −4.8 kcal/mol. The potential energy surface calculated for the *ortho*-addition and Cα−Cβ dissociation pathway of tyrosine is very similar to that of phenylalanine.

The potential energy surface calculated for *para*-addition and Cα−Cβ bond dissociation of tyrosine also resembles that of phenylalanine (Figure 9). The adduct formation is highly exothermic (−28.4 kcal/mol), and the addition transition state is about 5.8 kcal/mol lower in energy than the separated reactants. The energy barrier for the Cα−Cβ bond dissociation is about 26.8 kcal/mol. The overall reaction enthalpy change is −7.3 kcal/mol.

The OH loss from the *para*-addition intermediate is associated with a 21.5 kcal/mol energy barrier, which is much lower than that for Cα−Cβ bond dissociation. This may be one of the reasons why adduct-OH, rather than the side-chain abstraction product, is the major product for the reactions of tyrosine with radicals **a**−**c**. The overall enthalpy change for the addition and

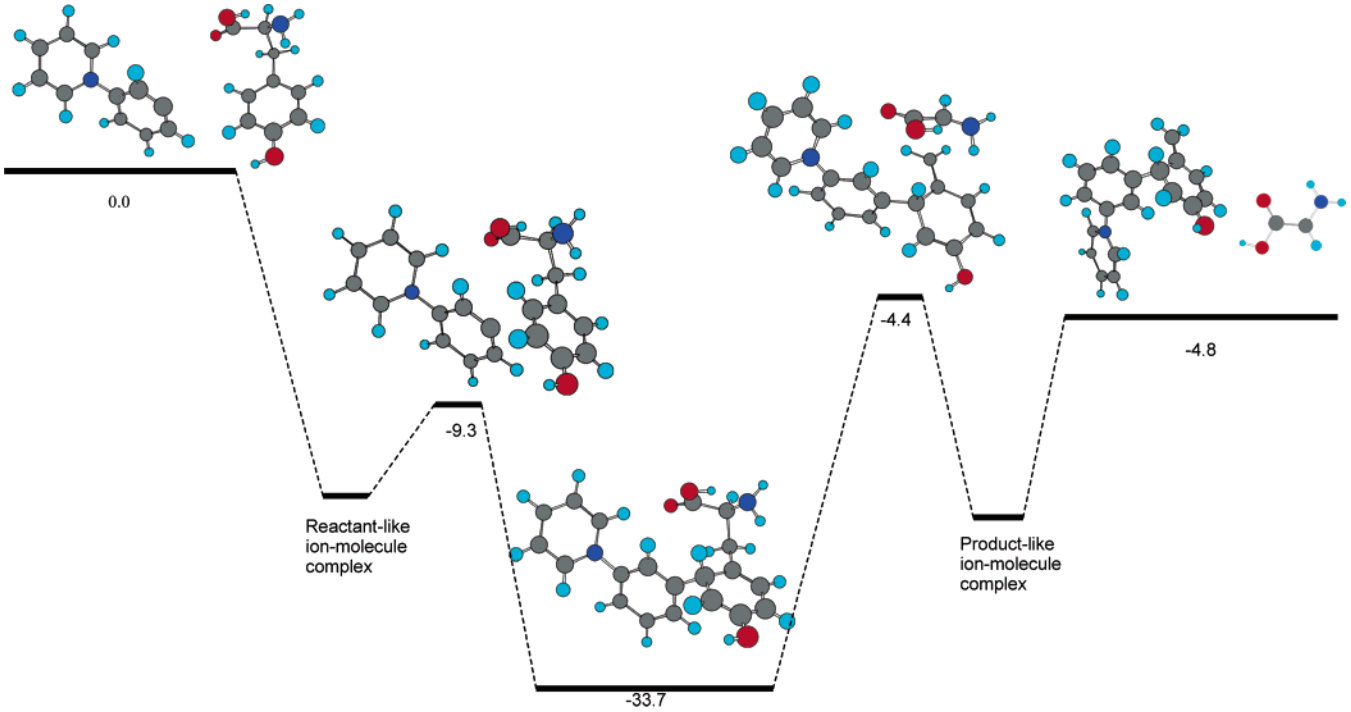

Figure 8. The potential energy surface (not scaled) for the addition of radical **c** to the *ortho*-position of tyrosine, followed by side-chain abstraction, as calculated at the B3LYP/6-31G (d)+ZPVE level of theory. All numbers are in kcal/mol.

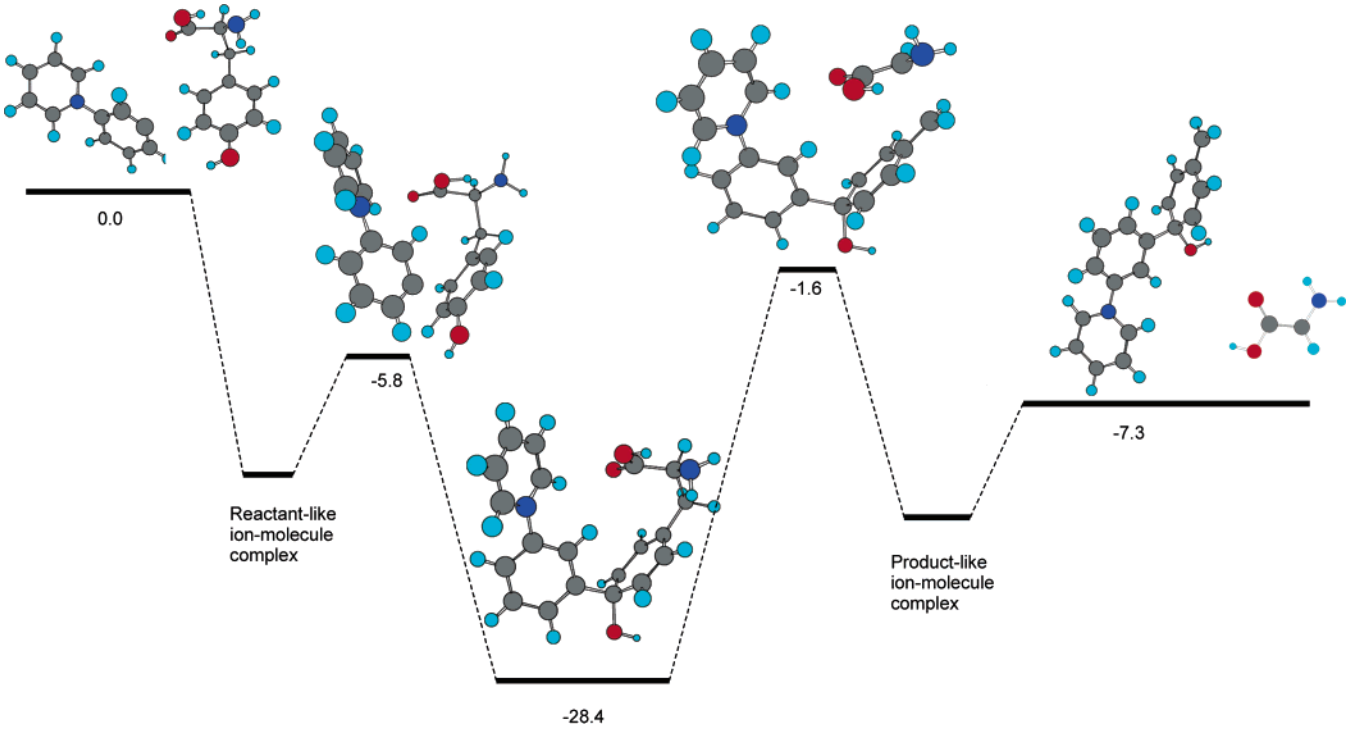

Figure 9. The potential energy surface (not scaled) for the addition of radical **c** to the *para*-position of tyrosine, followed by side-chain abstraction, as calculated at the B3LYP/6-31G (d)+ZPVE level of theory. All numbers are in kcal/mol.

OH loss pathway is −7.2 kcal/mol. The reaction is slightly less exothermic than the *para*-addition and Cα−Cβ bond dissociation pathway.

Reactions of Radicals a−c with Tryptophan. The reactions of tryptophan with radicals **a**−**c** (Table 3) also occur at nearly collision rate. Similar to the situation of phenylalanine, the accurate reaction efficiencies could not be determined. Hydrogen abstraction was observed for all radicals. The product branching ratios of hydrogen abstraction for typtophan are similar to those for phenylalanine, and lower than those for tyrosine. The main reaction pathway is addition to the 2-position of the indolyl functionality (the numbering scheme is given in Figure 2), followed by side-chain abstraction via Cα−Cβ bond cleavage. The corresponding side-chain abstraction product branching ratios are 67%, 64%, and 61% for radicals **a**, **b**, and **c**, respectively. These branching ratios are lower than those for

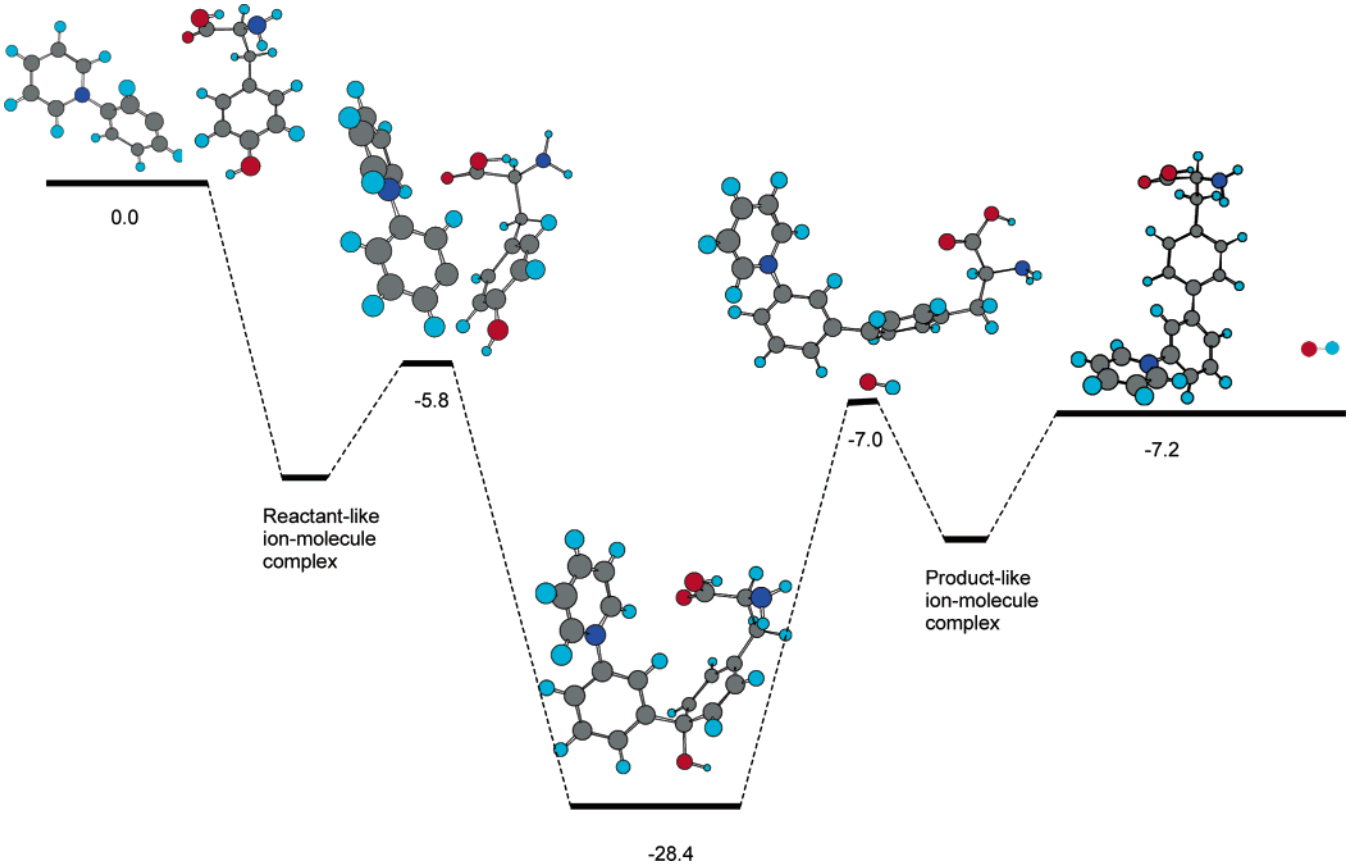

Figure 10. The potential energy surface (not scaled) for the addition of radical **c** to the *para*-position of tyrosine, followed by OH loss, as calculated at the B3LYP/6-31G (d)+ZPVE level of theory. All numbers are in kcal/mol.

Table 3. Product Branching Ratios[a] Measured for the Reactions of L-Tryptophan (MW = 204) with Radicals **a**−**c**

	product branching ratios (%)						
radical	hydrogen abstraction	adduct-X[b]	adduct-17	adduct-H	adduct	NH_2 abstraction	other ions
a	7	67	9	2	2	2	(*m*/*z* 271) 10[c]
b	6	64	0	5	14	0	(*m*/*z* 305) 11[c]
c	8	61	0	7	17	0	(*m*/*z* 271) 7[c]

[a] Product branching ratios are the average values of several experiments. [b] X = $NH_2CH{\cdot}COOH$. [c] The ions are likely to be adduct-X−CH_2, formed by *ipso*-radical addition with subsequent elimination of the β-alanyl radical.

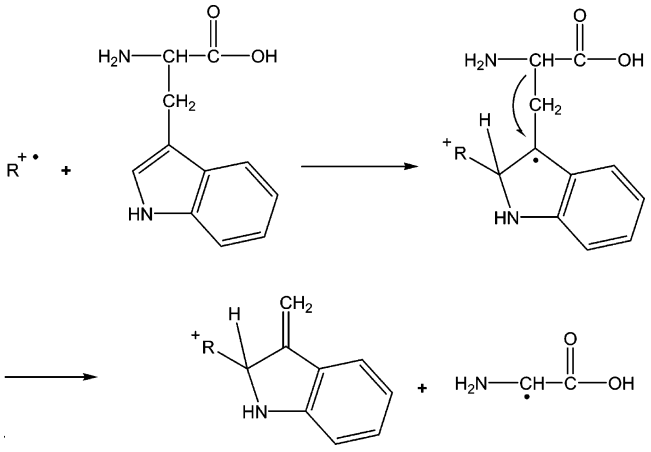

Figure 11. A possible mechanism for the addition of radicals **a**−**c** (represented by $R^{+\bullet}$) to tryptophan followed by side-chain abstraction.

phenylalanine (except for radical **a**), but much higher than those for tyrosine. A possible mechanism for the addition followed by side-chain abstraction is shown in Figure 11.

Conclusions

The reactions of radicals **a**−**c** with phenylalanine, tyrosine, and tryptophan are fast. The reaction efficiency ordering of radicals **a**−**c** toward tyrosine is in agreement with the electrophilicity ordering of the radicals, which in turn can be characterized by the radicals' electron affinity.[9]

Radicals **a**−**c** were found to abstract a hydrogen atom from all of the studied amino acids. The same reaction has been reported for HO• as well as for the neutral phenyl radical in solution.[1,8b] Amino group is abstracted from all of the amino acids by the most electrophilic radical **a**. This finding proves that the NH_2 abstraction observed previously[9] for highly electrophilic phenyl radicals upon reactions with simple amino acids also occurs for more complicated amino acids. To our best knowledge, this type of radical reaction has not been observed for the HO• radical.

The HO• radical has been reported to add to the phenyl ring of aromatic amino acids in solution.[1] There are no reports on the addition of neutral phenyl radical to amino acids. In this study, the radicals **a**−**c** were demonstrated to react with the

amino acids predominantly by addition to the aromatic ring followed by fragmentation. A novel reaction observed for all of the radicals with the amino acids is addition to the aromatic ring of the amino acid followed by Cα−Cβ bond cleavage that leads to side-chain abstraction by the radical. Both *ortho*- and *para*-addition can lead to this reaction. However, if addition occurs at the *para*-position in the phenyl ring of tyrosine, loss of OH is likely to take place. For tryptophan, the 2-position of the indolyl functional group is the only addition site that can lead to side-chain abstraction.

Acknowledgment. This research was supported by the National Institutes of Health.

JA044314O